

# Hertzian indentation of sintered alumina

M. T. LAUGIER

*Sandvik Limited, Hard Materials Research Centre, PO Box 109, Coventry, UK*

Hertzian indentation experiments have been performed on sintered  $\alpha$ -Al<sub>2</sub>O<sub>3</sub> using WC-Co spheres with radii in the range 0.5 to 6.5 mm. The critical load  $P^*$  to cause ring cracking was proportional to indenter radius  $R$  which is consistent with Auerbach's law. Values of room temperature fracture surface energy,  $\gamma$ , and fracture toughness,  $K_{IC}$ , were derived using the theories of Frank and Lawn and Warren.

## 1. Introduction

Early work on Hertzian indentation-induced fracture of brittle materials tended to focus on the empirical result known as Auerbach's Law [1] which states that the ratio of the critical load to produce a ring crack to the radius of the indenter is constant. In conjunction with Hertz's [2] equations (to be presented later), Auerbach's law implies that the maximum tensile stress at fracture is not constant but increases as  $R^{-1/3}$  where  $R$  is the indenter radius.

Developments in Hertzian indentation theory, based on the Griffith's [3] energy balance criterion, have led to improved understanding of ring crack formation in brittle materials and this has led to a convenient method for the determination of fracture surface energy,  $\gamma$ , and fracture toughness,  $K_{IC}$ . A brief account of these results is provided below.

When a spherical indenter is loaded against the flat surface of an elastic solid, a symmetrical stress distribution is set up in which the principal stresses are compressive in a tear-drop shaped region beneath the indenter to a depth of the order of the contact diameter. Outside the contact region, the greatest stress component is tensile and reaches its maximum value on the surface of the solid on the circle of contact. This tensile stress decreases rapidly in magnitude with both distance  $z$  from the surface and with distance  $y$  along the surface. Along the surface the stress is radial and may be written [2, 4]:

$$\sigma(y, z=0) = \frac{(1-2\nu)}{2\pi a^2} P \left(\frac{a}{y}\right)^2$$

where

$$a^3 = \frac{4kPR}{3E}$$

and

$$k = \frac{9}{16} \left[ (1-\nu^2) + (1-\nu^{12}) \frac{E}{E^1} \right]$$

where  $P$  is the normal load,  $a$  is the radius of the circle of contact,  $R$  the radius of the indenter,  $E, E^1$  and  $\nu, \nu^1$  are the Young's moduli and Poisson's ratios of the sample and indenter, respectively. The loading geometry is illustrated in Fig. 1.

Ring cracks are formed at a critical load  $P^*$  and generally it is found that the ring crack radius  $r$  is slightly greater than the contact radius  $a$ . Initially the crack is almost normal to the sample surface, but under increased loading it extends along a conical surface in a stable fashion remaining almost normal to the trajectory of maximum tensile stress.

The basis for a fracture mechanics treatment of Hertzian ring cracking has been the use of an expression for the stress intensity factor of an internal crack of length  $2c$  in an infinite plate subjected to a variable normal tensile stress along its length.

A general expression deduced by Warren [5] for the critical load  $P_c$  to form a ring crack from pre-existing flaws of size  $c$  is:

$$P_c = \frac{\beta k R \gamma}{(1-\nu^2)} \frac{a}{c} [\Phi(c)]^{-2}$$

where  $\Phi(c)$  represents an integral of the variable applied stress over the crack length  $c$ , and  $\beta$  is a

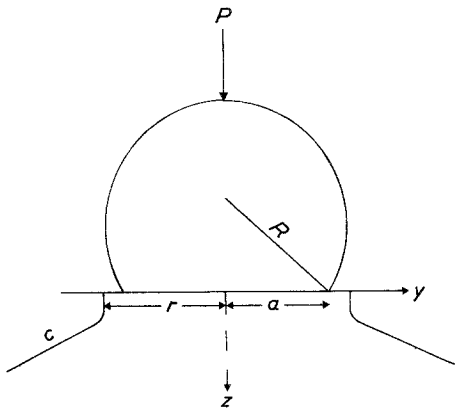


Figure 1 Illustration of Hertzian indentation loading geometry. A spherical indenter of radius  $R$  produces a contact radius  $a$  when loaded against a plane surface under a normal load  $P$ . Cracks of length  $c$  generally form outside the contact area at a radius  $r$ .

constant whose value is  $8\pi^3/27$  assuming the stress intensity factor for an internal crack of length  $2c$  to be applicable to the case of ring crack formation.

The expression  $\Phi(c)$  is a sensitive function of Poisson's ratio  $\nu$  and of the location of the ring crack relative to the contact radius. Curves of  $P_c$  against normalized crack length  $c/a$  are shown in Fig. 2 for the cases  $r/a = 1$  and  $r/a > 1$ .

When  $r/a = 1$ , the curve of  $P_c$  against normalized crack length  $c/a$  has two minima, and Frank and Lawn [6] considered this case to develop their theory of Hertzian ring cracks which leads to Auerbach's Law,  $P^*/R = \text{const.}$ , provided the flaw distribution does not contain flaws larger than those corresponding to the maximum in the

$P_c$  curve. Ring crack formation was considered to occur at all  $P_c$  values greater than the first  $P_c$  minimum, but only to become observable when  $P_c$  increases to its local maximum, when the crack becomes unstable and grows to an observable depth  $c^*$ . The value of  $P_c$  corresponding to the onset of crack growth is taken to correspond to the critical load written  $P^*$ . The corresponding value of flaw size,  $c^*$ , should represent an upper limit to observed flaw dimensions. Frank and Lawn give the approximate result

$$P^* = 2.3 \times 10^4 \times \frac{Rk\gamma}{(1-\nu^2)(1-2\nu)^2}.$$

However, ring cracks generally form for  $r/a > 1$ , when the  $P_c$  curve has only one minimum. In this case, Warren considers ring crack formation to occur at the value of  $P_c$  corresponding to the minimum, and again the details of the flaw distribution are not significant, provided sufficient flaws are present in the range corresponding to the  $P_c$  minimum. The observed critical load  $P^*$  is now considered to correspond to the  $P_c$  minimum.

Previous determinations of fracture surface energy by this technique have been made for ZrC, VC and WC [5], TiC [5, 7], UO<sub>2</sub> [8], ThO<sub>2</sub> [9].

## 2. Experimental procedure

Specimens were Feldmuhle SN60 cold-pressed and sintered  $\alpha$ -Al<sub>2</sub>O<sub>3</sub> cutting tips containing 4 wt % ZrO<sub>2</sub>, of grain size 2  $\mu\text{m}$ , and dimensions 13 mm  $\times$  13 mm  $\times$  7 mm. The surfaces were lapped and polished using 2  $\mu\text{m}$  diamond paste. The indenters were sintered WC-Co spheres with radii in the range 0.5 to 6.5 mm. Loading was performed by

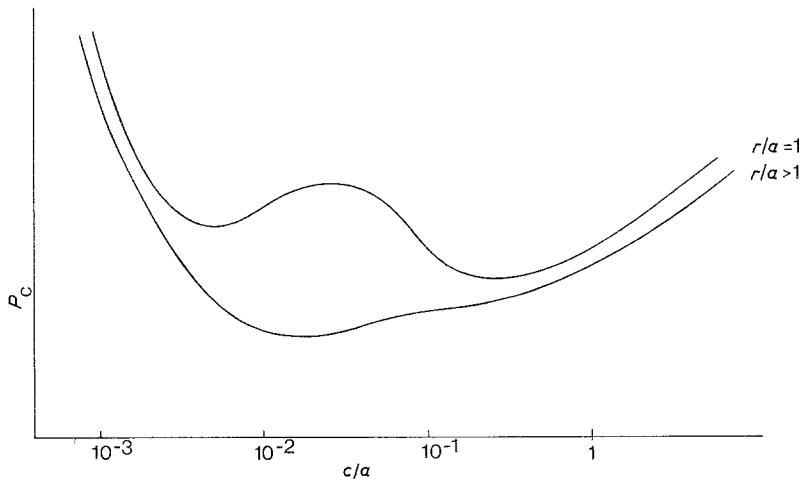


Figure 2 Curves of  $P_c$  against normalized crack length  $c/a$  for  $r/a = 1$  and  $r/a > 1$ .

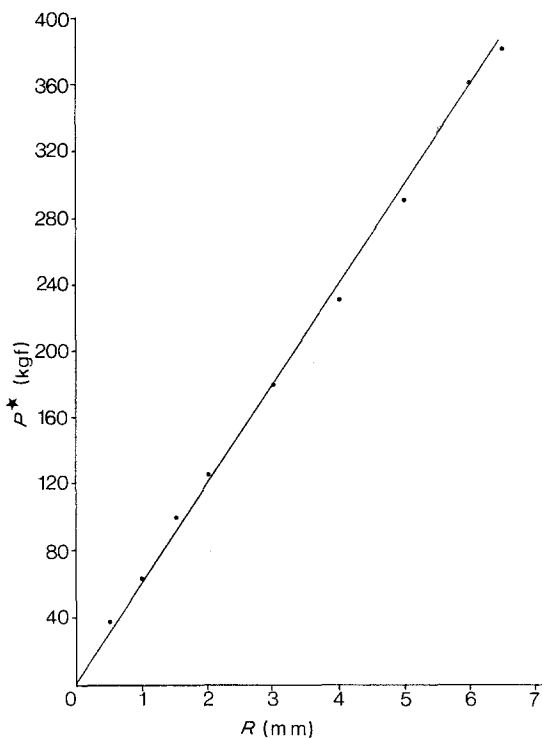


Figure 3 Critical load  $P^*$  to produce ring cracks plotted against indenter radius  $R$ .

means of a Mayes 100 kN Universal Mechanical Testing Machine using a loading rate of  $300 \text{ kgf min}^{-1}$ . The critical load for cracking was determined for each indenter radius by progressively increasing the applied load until cracks forming at least 50% of a complete circle were observed. Indenters were lightly smeared with grease to enable determination of the contact area. Observations were carried out using an optical microscope and crack radius  $r$  and contact radius  $a_g$  were determined using a micrometer eyepiece. Some indication of plastic deformation was observed for small overloaded indenters with radii  $R < 3 \text{ mm}$ . Indenters were examined after loading but were not found to be damaged.

### 3. Results

Critical load  $P^*$  to produce ring cracks for indenter radii  $R$  in the range 0.5 to 6.5 mm is shown plotted against  $R$  in Fig. 3. The observed linear relationship is consistent with Auerbach's law. Fig. 4 shows calculated contact radius  $a$  plotted against measured grease patch radius  $a_g$ . The grease patch radius  $a_g$  was found to be consistently greater than the contact radius  $a$ , calculated from the Hertz theory, with  $a_g = 1.14a$ .

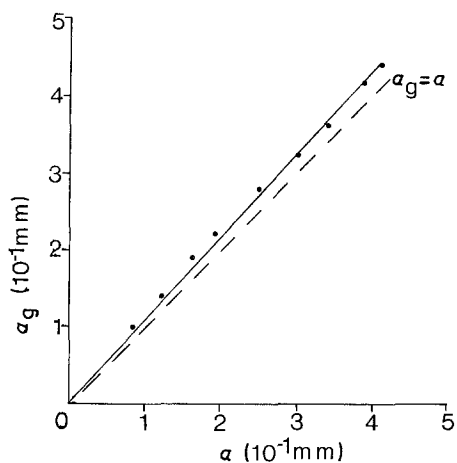


Figure 4 Measured grease patch radius  $a_g$  plotted against calculated contact radius  $a$ .

Similar effects have been observed using the grease ring technique for silicate glass using steel indenters [10], and for  $\text{UO}_2$  [8] and  $\text{ThO}_2$  [9] using hardened steel spheres where elastic mismatch is small. Recent low load ( $P < 1 \text{ kg}$ ) measurements using an accurate Newton's rings technique for fused silica, soda-lime glass and sapphire indented with steel and WC spheres also showed a similar effect [11]. Soda-lime glass indented with steel spheres was an exception in that measured and calculated values were in close agreement. It would thus appear that Hertzian theory in most cases underestimates the experimental contact radius. However, the reliability of the grease ring method in providing a true measure of contact radius is unknown; this could be investigated using the Newton's rings method. Measured crack radius,  $r$ , is shown plotted against calculated contact radius,  $a$ , in Fig. 5. Cracks form consistently outside the contact region and from the graph  $r/a = 1.21$ . If the grease radius  $a_g$  is taken to represent the contact radius, then the results should be evaluated in terms of the ratio  $r/a_g = 1.06$ . Both approaches are considered.

In the theory of Warren, the critical load to form ring cracks corresponds to the minimum of the crack extension function  $(a/c)(\Phi)^{-2}$ . From the data of Warren, the locus of the minima of  $(a/c)(\Phi)^{-2}$  with respect to normalized crack length  $c/a$  was constructed as a function of  $r/a$  for alumina, for which Poisson's ratio was taken as  $\nu = 0.237$ , and is shown in Fig. 6 [12]. The mechanical data required is collected in Table I. Fig. 7 is an SEM micrograph of the polished alumina surface.

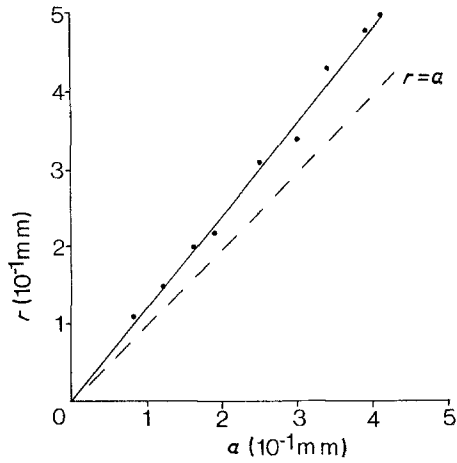


Figure 5 Measured crack radius  $r$  plotted against calculated contact radius  $a$ .

#### 4. Discussion

These results enable room temperature fracture surface energy  $\gamma$  and fracture toughness  $K_{IC}$  to be determined. The Auerbach constant  $P^*/R = 590 \text{ kN m}^{-1}$  from the slope of Fig. 3.

From the theory of Warren,

$$\frac{P^*}{R} = \frac{\beta\gamma k}{1-\nu^2} \frac{a}{c} (\Phi)^{-2}$$

taking the value of  $(a/c)(\Phi)^{-2}$  from Fig. 6, when  $r/a = 1.21$  from Fig. 5 leads to a value of  $\gamma = 49 \text{ J m}^{-2}$ , where the value of  $\beta = 8\pi^3/27$  used is that for an internal crack of length  $2c$ .

If the grease radius  $a_g$  is taken as the true contact radius, a consistent approach which remains within the analytical framework is to think of  $a_g$  as resulting from the observed critical load  $P^*$  but with a larger effective indenter radius  $R' > R$ . The grease radius may then be calculated from Hertzian theory,  $a_g = a(R')$ . The relation

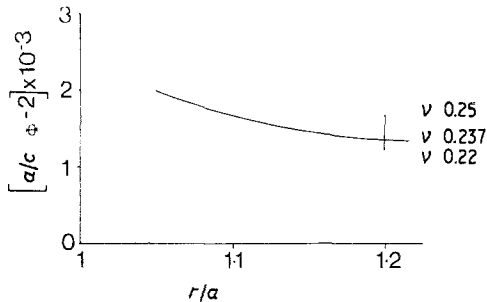


Figure 6 Locus of minima with respect to normalized crack length  $c/a$  of the crack extension function  $a/c(\Phi)^{-2}$  constructed as a function of  $r/a$ .

TABLE I Mechanical data

Material	Young's modulus $E$ ( $10^5 \text{ MN m}^{-2}$ )	Poisson's ratio, $\nu$
$\text{Al}_2\text{O}_3$	3.7	0.237
WC-Co	6.0	0.25

for the fracture surface energy is accordingly rewritten as

$$\gamma = \frac{4}{3} \frac{(1-\nu^2)}{\beta E a^3} \frac{c}{a} (\Phi)^2 P^{*2}$$

It is noted that whenever  $a_g = a(R') > a(R)$  then a reduced value of  $\gamma$  will be obtained. This procedure may be thought of as providing bounds for the fracture surface energy  $\gamma$ . The new value of fracture surface energy obtained using  $a_g = a(R')$ , and the value of  $(c/a)(\Phi)^2$  for  $r/a = 1.06$  from Fig. 6 is  $\gamma = 24 \text{ J m}^{-2}$ .

From the Frank and Lawn theory:

$$\frac{P^*}{R} = 2.3 \times 10^4 \frac{k\gamma}{(1-\nu^2)(1-2\nu)^2}$$

and this leads to a value of  $\gamma = 7.5 \text{ J m}^{-2}$ .

Ring crack formation requires a pre-existing distribution of surface flaws with which the Hertzian stress field can interact. The normalized size of required pre-existing flaws is of the order of  $c/a \sim 3 \times 10^{-2}$ . Since  $0.1 \text{ mm} \leq a \leq 0.4 \text{ mm}$  from Fig. 4, the range of required pre-existing surface flaws is  $3 \mu\text{m} \leq c \leq 12 \mu\text{m}$ . From the micrograph of Fig. 7 it is seen that flaws are present throughout the required range, but that relatively few are to be found near the upper size limit.

The Frank and Lawn theory requires pre-existing flaws in the range  $1 \times 10^{-2} \leq (c/a) \leq 1 \times$

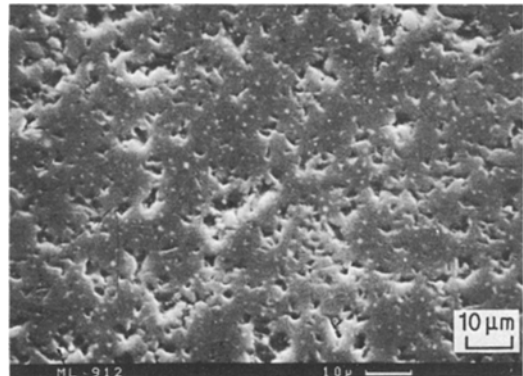


Figure 7 SEM micrograph of polished alumina surface.

$10^{-1}$ , which is equivalent to  $1 \mu\text{m} \lesssim c \lesssim 40 \mu\text{m}$ . In the samples examined flaw sizes  $c > 10 \mu\text{m}$  were infrequent.

Fracture toughness,  $K_{1C}$ , is found from the linear fracture mechanics relation:

$$2\gamma = \frac{1-\gamma^2}{E} K_{1C}^2.$$

Warren's theory leads to  $K_{1C} = 6.2 \text{ MN m}^{-3/2}$  using calculated values of the contact radius, and  $K_{1C} = 4.3 \text{ MN m}^{-3/2}$  when contact is assumed to be given by the grease patch radius. The corresponding result from the Frank and Lawn expression is  $K_{1C} = 2.5 \text{ MN m}^{-3/2}$ . The  $K_{1C}$  values obtained from Warren's theory fall either side of the manufacturer's value\* given as  $K_{1C} = 5.5 \text{ MN m}^{-3/2}$  ( $\gamma = 38 \text{ J m}^{-2}$ ), whilst the result obtained from the Frank and Lawn expression is significantly lower. The results obtained from Warren's theory are in general agreement with published results on similar grain size materials [13, 14]. The recent results of Lange [14], obtained by an indentation technique [15] on  $\text{Al}_2\text{O}_3\text{-ZrO}_2$  materials with grain size in the region of  $2 \mu\text{m}$ , are of particular interest. Lange finds toughness values  $K_{1C} = 5.0 \text{ MN m}^{-3/2}$  for pure  $\text{Al}_2\text{O}_3$  and  $K_{1C} = 5.9 \text{ MN m}^{-3/2}$  for  $\text{Al}_2\text{O}_3\text{-7.5 vol\% ZrO}_2$ . His extrapolated curve gives a value  $K_{1C} = 5.3 \text{ MN m}^{-3/2}$  for  $\text{Al}_2\text{O}_3\text{-3 vol\% ZrO}_2$  which is the composition of the present material as a volume percent.

## 5. Conclusion

These results provide good confirmation of Warren's theory in its original form. When the grease patch

radius is taken as the contact radius, the resulting toughness value falls below that for pure  $\text{Al}_2\text{O}_3$  of similar grain size. However, the relationship between the grease patch radius, the true contact radius and the calculated radius from Hertzian theory, remains to be elucidated. The toughness value for this material obtained from the Frank and Lawn expression is significantly lower.

## References

1. F. AUERBACH, *Ann. Phys. Chem.* **43** (1981) 61.
2. H. HERTZ, "Hertz's Miscellaneous Papers" (Macmillan, London, 1896).
3. A. A. GRIFFITH, *Phil. Trans. Roy. Soc. A* **221** (1920) 163.
4. S. TIMOSHENKO and J. N. GOODIER, "Theory of Elasticity", 2nd Edn. (McGraw-Hill, New York, 1951).
5. R. WARREN, *Acta Metall.* **26** (1978) 1759.
6. F. C. FRANK and B. R. LAWN, *Proc. Roy. Soc. A* **299** (1967) 291.
7. B. D. POWELL and D. TABOR, *J. Phys. D Appl. Phys.* **3** (1970) 783.
8. HJ MATZKE and R. WARREN, *J. Nucl. Mat.* **91** (1980) 205.
9. HJ MATZKE, *J. Mater. Sci.* **15** (1980) 739.
10. J. P. A. TILLET, *Proc. Phys. Soc.* **B69** (1956) 47.
11. M. M. CHAUDHRI and E. H. YOFFE, *Phil. Mag.* **A44** (1981) 667.
12. W. R. DAVIS, *Trans. Brit. Ceram. Soc.* **67** (1968) 515.
13. N. CLAUSSEN, B. MUSSLER and M. V. SWAIN, *J. Amer. Ceram. Soc.* **65** (1982) c-14.
14. F. F. LANGE, *J. Mater. Sci.* **17** (1982) 247.
15. A. G. EVANS and E. A. CHARLES, *J. Amer. Ceram. Soc.* **59** (1976) 371.

Received 31 January  
and accepted 18 May 1983

\*Obtained using a single edge notched beam technique.